Volume 22
Number 41
7 November 2020
Pages 6741–6948

CrystEngComm

rsc.li/crystengcomm

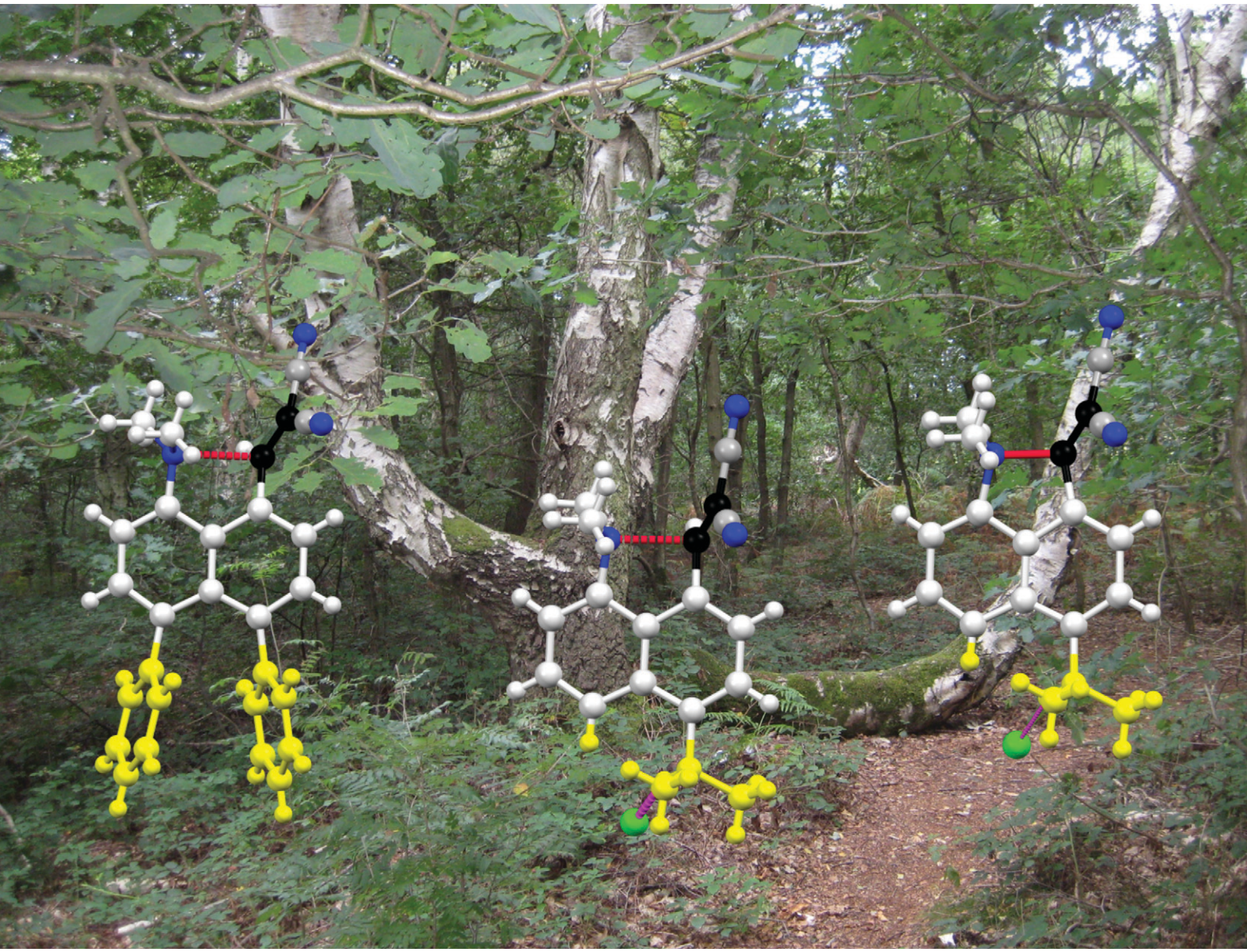

ISSN 1466-8033

ROYAL SOCIETY OF CHEMISTRY

PAPER

John D. Wallis *et al.*

Modelling of an aza-Michael reaction from crystalline naphthalene derivatives containing *peri–peri* interactions: very long N–C bonds?

CrystEngComm

PAPER

View Article Online
View Journal | View Issue

Cite this: *CrystEngComm*, 2020, **22**, 6783

Modelling of an aza-Michael reaction from crystalline naphthalene derivatives containing *peri–peri* interactions: very long N–C bonds?†

Jonathan C. Bristow,[a] Isaac Naftalin,[a] Stacey V. A. Cliff,[a] Songjie Yang,[a] Marina Carravetta,[b] Ivo Heinmaa,[c] Raivo Stern[c] and John D. Wallis*[a]

Received 4th August 2020,
Accepted 16th September 2020

DOI: 10.1039/d0ce01137a

rsc.li/crystengcomm

The separation between a pair of *peri*-located dimethylamino and ethene-2,2-dinitrile groups in a naphthalene molecule, which models the progress of a Michael reaction, can be controlled by the installation of a short ethylene bridge or the introduction of repulsive interactions at the opposite set of *peri* positions. Introduction of a dimethylammonium substituent produced a hydrated chloride salt in which the $Me_2N\cdots C(H){=}C(CN)_2$ separation between reactive groups decreases, reversibly, from 2.167 Å at 200 K to 1.749 Å at 100 K, with the maximum rate of change in the range 128–140 K, which was studied by variable temperature X-ray crystallography and solid state NMR. From these and other crystallographic data a correlation between $Me_2N\cdots C$ bond formation and alkene bond breaking was constructed for the first step of an aza-Michael reaction.

Introduction

Bond formation and breaking is a core theme in chemical reactivity but it is very difficult to monitor the whole process, including the correlation between bond formation and breaking, due to the high energy of the transition state which involves partially broken and formed bonds. Indeed transition states have only been accessed experimentally by femtosecond spectroscopy as demonstrated by Zewail,[1] and calculations offer a more pragmatic approach to exploring transition state structures.[2] The Michael reaction is a very well-known reaction, involving the addition of a nucleophile such as an amine, thiolate or enolate, to an electron deficient alkene or alkyne. It is used to prepare a wide variety of substances including enantiopure ones, and may be promoted, for example, by organocatalysis.[3] The aza-Michael reaction, in particular, is used in the construction of heterocycles, alkaloids and molecules of pharmaceutical relevance.[4] Some calculations of the transition states structures and/or energies for such reactions have been reported, in some cases aimed at predicting mutagenicity of the Michael acceptor.[5,6]

The idea of modelling reaction pathways based on structural data from crystals is well established for both organic and some inorganic systems though the experimental data generally lies closer to the start or end of the reaction process.[7] The naphthalene framework has been used for observing interactions and reactions between pairs of groups placed at the *peri*-positions by crystallographic and solid-state NMR methods.[8] Apart from nucleophile/electrophile interactions, *peri*-substituted naphthalenes have provided chiral hydrocarbons with very large steric interactions,[9] frustrated lone pairs systems[10] and proton sponges,[11] with experimental charge density studies carried out in selected cases.[12] Attractive interactions between functional groups were first reported in the pioneering work from Dunitz *et al.* on the interactions of nucleophiles with carbonyl groups as in naphthalene **1**.[13] Such n–π* interactions affect the chemistry of the electrophile, for example the aldehyde **2** both protonates and acylates on the O atom with formation of a N–C bond between the two groups,[14] as do several closely

[a] *School of Science and Technology, Nottingham Trent University, Clifton Lane, Nottingham NG11 8NS, UK. E-mail: john.wallis@ntu.ac.uk*
[b] *School of Chemistry, University of Southampton, Highfield, Southampton, SO17 1BJ, UK*
[c] *Laboratory of Chemical Physics, National Institute of Chemical Physics and Biophysics, Tallinn, Estonia*

† Electronic supplementary information (ESI) available. CCDC 2016747–2016754 and 2019629. For ESI and crystallographic data in CIF or other electronic format see DOI: 10.1039/d0ce01137a

related ketones.[15] We have reported the structure of a series of compounds where a dimethylamino group lies next to a polarised alkene, such as **3** and **4**.[16] In the first of these the nucleophile impinges on an alkene terminated by two nitriles with a $Me_2N\cdots C$ separation of 2.413(2) Å while in the latter case, where the alkene is activated by two in-plane lactone carbonyls, the groups reacts to form a zwitterion with a long Me_2N–C bond of 1.651(3) Å. Although a range of such systems has been studied,[17] no such structures with $Me_2N\cdots C$ separations in the range 1.7–2.4 Å have been found. Indeed, the only molecular structure with such N⋯C separations are for transannular interactions across the ring systems of particular alkaloids, such as clivorine **5** (1.93 Å) and senkirkine **6** (2.25 Å),[18] as highlighted by Bürgi, Dunitz and Schefter.[19] n–π* interactions between peptide carbonyls have been particularly highlighted recently for their role in determining the conformation of proteins.[20]

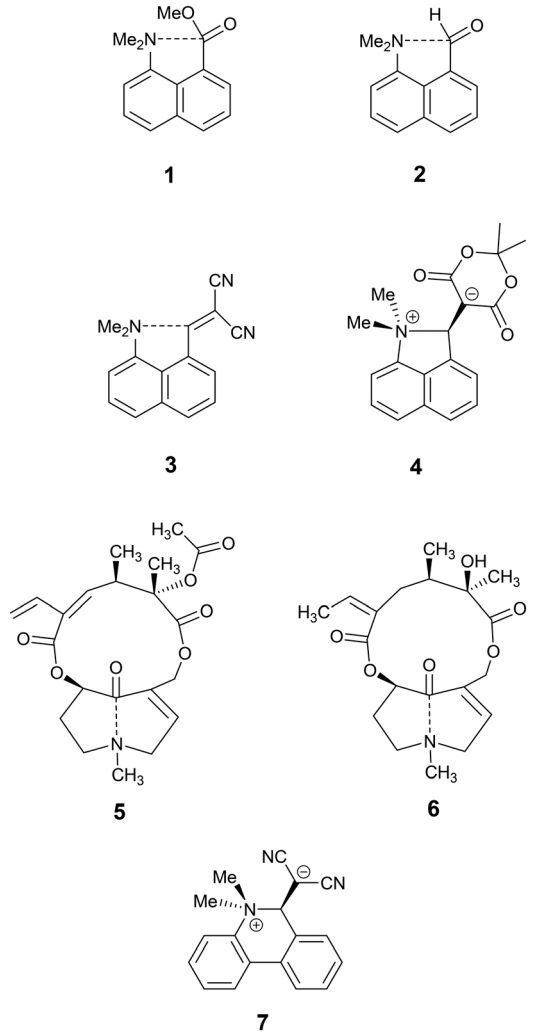

To modify *peri*-interactions and find such intermediate separations between the *peri*-groups, we decided to explore whether a pair of substituents at the second set of *peri*-positions of the naphthalene skeleton could control the electrophile/nucleophile separation at the first pair. In particular, would repulsion between a second pair of substituents lead to the first pair being pushed closer together, and conversely would contraction at the second pair lead to an increased electrophile/nucleophile separation? We describe here results for compounds containing a dimethylamino group and a dicyanoethenyl group as the nucleophile/electrophile pair. The results of a reaction between this pair of groups to form a zwitterion has been observed in crystals of the corresponding biphenyl system **7**, with new Me_2N–C bonds of 1.586(3) and 1.604(3) Å in the two independent molecules.[21] In this case the reaction involves the formation of a less strained ring than in the naphthalene series.

Discussion

Structural effects of a second set of *peri*-substituents in a naphthalene derivative

We started by exploring the effect of installing an ethylene bridge between the second set of *peri*-positions on the $Me_2N\cdots C(H){=}C(CN)_2$ separation by studying acenaphthene derivative **8**. The molecule was prepared from acenaphthene in six steps (ESI†). Its X-ray crystal structure, determined at 150 K, showed that the installation of the ethylene bridge had led to a significant increase in the distance between the functional groups: the $Me_2N\cdots CH{=}C(CN)_2$ distances in the two crystallographically unique molecules are 2.755(2) and 2.846(2) Å compared to 2.413(2) Å in the unsubstituted analogue **3** (Fig. 1). Furthermore, the difference of 16–17° in the *exo* angles at the fusion the benzene rings between the two *peri* positions (ϕ and ψ in Table 1) shows how the widening of the ϕ angle between the amino and alkene groups has been caused by the compression of the ψ angle which was imposed by the short ethylene bridge: *i.e.* ϕ: 127.30(18)/128.54(17)° *vs.* ψ: 111.73(17)/111.25(18)°. In **3**, without the ethylene bridge, these two angles differ only by *ca.* 2° (122.6(2) and 120.42(12)°). The increased separation, and reduced n–π* interaction between the –NMe_2 and –$C(H){=}C(CN)_2$ groups, allows the electrophilic group in one of the two crystallographically independent molecules to rotate closer to the acenaphthene plane and to increase the conjugation between the alkene and the aromatic system. Indeed, this general strategy of a short *peri*-bridge was also implemented in the design of acenaphthylene derivative **9** by Ishigaki and Suzuki which shows an exceptionally long C–C bond between *peri*-substituents[22] and also in materials with frustrated lone pairs such as **10**.[10]

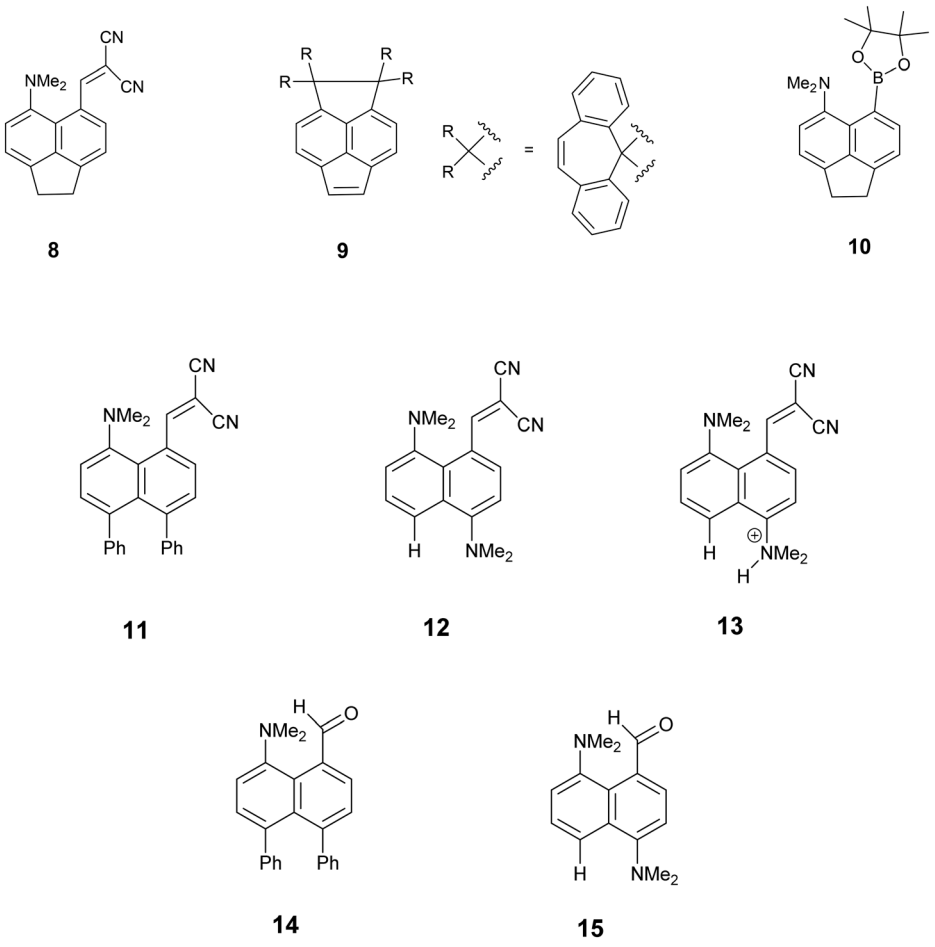

To explore the opposite effect, the ethylene bridge was replaced by two phenyl rings which should repel each other since the *peri*-naphthalene ring carbon atoms are only *ca.* 2.5 Å apart. Thus, the *peri*-diphenyl derivative **11** with a $Me_2N\cdots C(H)=C(CN)_2$ interaction at the opposite *peri*-positions was prepared from 1,8-diphenylnaphthalene in five steps *via* aldehyde **14**, and the dinitrile **11** was crystallised as a toluene solvate. The X-ray crystal structure was determined and the molecular structure is shown in Fig. 2. The two phenyl groups are tilted at 62.2 and 63.2° to the naphthalene, and they are repelled apart with an angle of 20.9° between them and a widening of the nearby *exo*-angle (ψ) at the fusion of the naphthalene rings to 126.24(13)°. The opposite *exo*-angle (ϕ) is compressed to 117.74(12)° leading to the other two *peri* groups being oriented closer together so that the $Me_2N\cdots C(H)=C(CN)_2$ separation is reduced to 2.3603(19) Å, 0.053 Å shorter than in the dinitrile **3** without *peri* phenyl groups.

Continuing the idea of introducing a repulsive *peri*-interaction, the corresponding naphthalenes with just one $-NMe_2$ group, unprotonated or protonated, in the opposite *peri*-position, **12** and **13·Cl** respectively, were prepared. Protonation was expected to increase the effective size of the dimethylamino group. Compound **12** was prepared by *peri*-lithiation of 1,5-bis(dimethylamino) naphthalene and treatment with DMF to yield aldehyde **15** followed by Knoevenagel condensation with malonitrile. The X-ray structure of the unprotonated material **12** (Fig. 2) shows that the *peri*-repulsion between the H and $-Me_2N$ groups in the two crystallographically unique molecules is not very effective, even though there is van der Waals contact between the *peri* H atom and a *N*-methyl H atom. The *exo* angles at the fusion of the benzene rings differ only by *ca.* 2°, and are similar to those in naphthalene **3** which has no second dimethylamino group. The $Me_2N\cdots C$ interactions are just slightly longer than in **3** (Table 1). The results from the X-ray crystal structure of the HCl salt, however, showed a much more significant repulsion between the dimethylammonium group and the *peri* H atom.

Variable temperature *peri*-interactions in 13·Cl

The salt **13·Cl**, readily prepared from **12**, crystallised in the orthorhombic space group *Fdd*2 with one molecule of water per two cations of **13** and two chloride anions. In the crystal structure of this salt at 200 K the cation shows a remarkably short $Me_2N\cdots C(H)=C(CN)_2$ interaction of just 2.167(4) Å, which is *ca.* 1 Å within the separation predicted by the sum

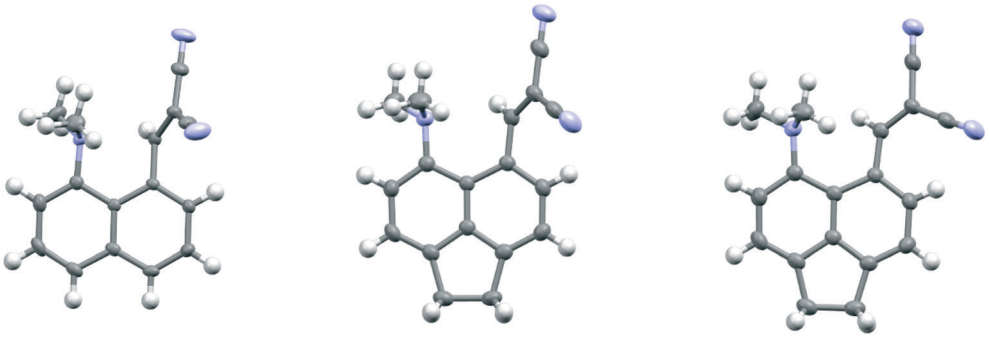

Fig. 1 Molecular structures of **3**[16] (left) and the two independent molecules of **8** (middle and right) in the second of which (right) the alkene has rotated to be closer to the naphthalene plane.

of van der Waals radii (Fig. 3). This is also *ca.* 0.25 Å shorter than is observed in the corresponding naphthalene derivative **3** with just a pair of H atoms at the second set of *peri*-positions. The dimethylamino group is well aligned with the alkene-dinitrile group for a reaction to take place, with a $Me_2N\cdots C{=}C$ angle of 113.2(2)°. Furthermore, the alkene bond is lengthened by 0.015 Å compared to the unsubstituted molecule **3**, suggesting that there has been a small degree of progress along the reaction coordinate for the addition of a tertiary amine the alkene. At the other side of the molecule the dimethylammonium substituent and *peri*-H atom are repelled apart, so there is van der Waals contact (2.07 Å) between the N–H and the *peri*-H atom. The *N*-methyl groups lie to either side of the naphthalene plane to minimise steric

Table 1 Selected molecular geometry for naphthalenes **3**, **8**, **11** and **12** and cation **13**

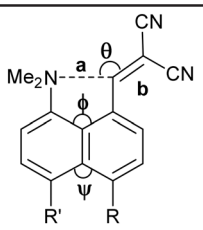

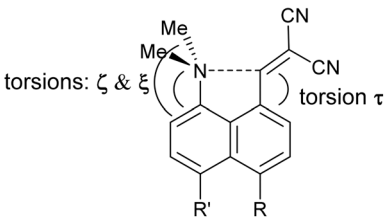

Compound	*T*/K	*a*/Å	*b*/Å	*θ*/°	$Me_2NH\cdots H$/Å
3, R = R′ = H	150	2.413(2)	1.354(2)	112.5(2)	—
8, R,R′ = CH_2CH_2	150	2.755(2) 2.846(2)	1.343(3) 1.348(3)	122.71(14) 133.00(15)	—
11, R = R′ = Ph	150	2.3603(19)	1.356(2)	114.21(11)	—
12, R = NMe_2, R′ = H	150	2.455(2) 2.512(2)	1.356(2) 1.350(2)	116.29(12) 117.19(12)	—
13·Cl, R = $^+NHMe_2$, R′ = H	200 150 134 100	2.167(4) 2.098(4) 1.932(4) 1.749(3)	1.369(4) 1.378(4) 1.401(4) 1.431(3)	113.2(2) 113.4(2) 115.0(2) 115.9(2)	2.07 2.09 2.11 2.14

	T/K	*φ*/°	*ψ*/°	*τ*/°	*ζ*/°	*ξ*/°
3, R = R′ = H	150	120.42(14)	122.6(2)	56.5(2)	49.7(2)	−81.5(2)
8, R,R′ = CH_2CH_2	150	127.30(18) 128.54(17)	111.73(17) 111.25(18)	51.9(3) 35.9(3)	45.8(2) 27.5(3)	−82.1(2) −100.8(2)
11, R = R′ = Ph	150	126.24(13)	117.74(12)	51.0(2)	94.95(18)	−36.9(2)
12, R = NMe_2, R′ = H	150	120.27(15) 120.81(15)	122.74(15) 122.75(15)	53.1(2) 49.9(2)	77.8(2) 90.5(2)	−54.9(3) −43.0(3)
13·Cl R = $^+NHMe_2$, R′ = H	200 150 134 100	117.8(2) 117.1(2) 116.0(2) 114.3(2)	126.5(3) 127.1(2) 128.1(2) 129.3(2)	53.0(4) 51.4(4) 46.4(4) 42.0(4)	48.9(5) 49.1(4) 49.6(4) 48.0(3)	−82.3(4) −81.0(3) −78.6(3) −76.4(2)

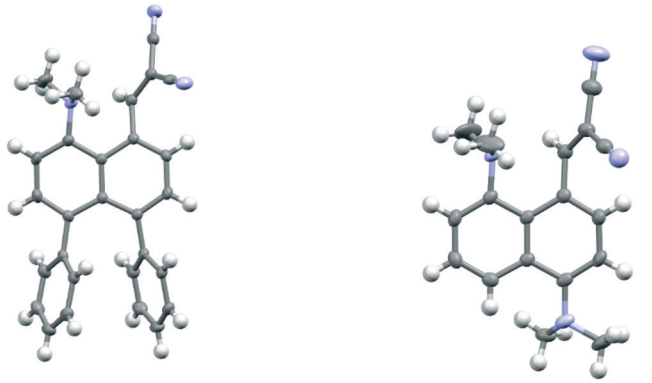

Fig. 2 Molecular structures of naphthalene **11** with two *peri* phenyl groups (left) and one of the two crystallographically unique molecules of naphthalene **12** with a dimethylamino group and hydrogen atom at the second set of *peri*-positions (right).

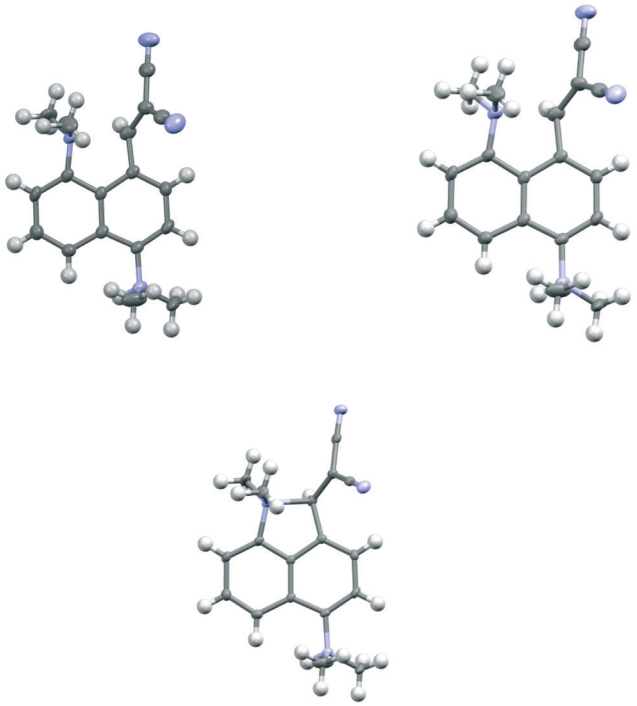

Fig. 3 The molecular structure of the cation **13** at 200 K (top left), at 150 K (top right) and 100 K (below), with $Me_2N\cdots C$ separations of 2.167(4), 2.098(4) and 1.749(3) Å respectively. A bond between the functional groups is drawn in the latter case, to indicate the closer distance.

interaction with the *ortho* H atom. This *peri*-repulsion leads to an *exo* angle ψ of 126.5(3)° and consequentially to a much smaller *exo* ϕ angle of 117.8(2)°, and the closer approach between the dimethylamino group and alkene. In the crystal structure the dimethylammonium group forms a hydrogen bond to the chloride anion, and a water molecule bridges two chloride anions (Fig. 4). Pairs of cations of **13**, linked by hydrogen bonding through a Cl···HOH···Cl unit, lie in columns along the *b* axis, with four parallel columns lying side by side along the *a* axis (44.4094 Å at 200 K). The two cations are related by the two fold axis along the short *c* axis which cuts the water's oxygen atom. The column is completed by a second such pair, related to the first by a two-fold screw axis along the *c* axis (Fig. 4, *vide infra*).

On cooling the crystal of this salt to 150 K the molecular structures changes by a small amount, with the $Me_2N\cdots C{=}C$ distance contracting by 0.069 Å to 2.098(4) Å, and the alkene lengthening slightly by 0.009 Å. However, on cooling further to 100 K the structure of the cation underwent a more significant change. The contraction of the crystal lattice applies pressure to the cation, and the dimethylamino and dicyanoethenyl groups are pushed closer together to give a $Me_2N\cdots C$ separation of 1.749(3) Å, though this is still not as short as in the biphenyl derivative **7** (1.586/1.604 Å). The alkene bond has also partly broken and its length (1.431(3) Å) lies intermediate between that for this species at 200 K (1.369 Å), and that in the biphenyl case **7** (1.487/1.493 Å). Furthermore, the molecular geometry at the attacked alkene carbon has changed from planar to partially tetrahedral. The coordinates of the hydrogen atom at this centre were found in a difference Fourier map and refined in the X-ray analysis. Thus the angles between the two C–C bonds and the C–H bond at this centre change from 122.2, 116.2, 117.9° at 200 K to 118.6, 112.7 and 109.6° at 100 K. As this addition reaction proceeds partial charges, positive and negative, should develop respectively on the dimethylamino nitrogen atom and on the carbon atom between the nitrile groups. The *N*-methyl bonds have lengthened in response, from 1.462(5) and 1.476(4) Å at 200 K to 1.486(3) and 1.490(3) Å at 100 K. These four values lie in-between those for naphthalenes **3** and **4**, 1.459 and 1.502 Å respectively, which have longer and shorter $Me_2N\cdots C$ separations (2.413 and 1.651 Å).[16] There is also a tightening of the bond angles at the N atom in the dimethylamino group on going from 200 K to 100 K. The bonds from the developing carbanion to the nitrile groups have shortened from 1.430(4) and 1.434(4) Å at 200 K to 1.416(3) and 1.423(3) Å at 100 K, with slight increases in the nitriles' bond lengths: from 1.135(4)/1.142(4) Å to 1.149(3)/1.149(3) Å, as the nitriles play a greater role in stabilising the negative charge. All these changes are consistent with progress along the reaction coordinate on cooling the crystal. Overall, this suggests that there is a partially formed bond of length 1.749 Å between the two functional groups. The $Me_2N\cdots C$ interaction is aligned approximately along the *c* axis of the cell, and this axis contracts by *ca.* 2.8% on cooling from 200 K to 100 K, while there are much smaller changes on the *a* axis (+0.6%) and the *b* (−0.7%). The overall packing arrangement observed at 200 K is maintained (Fig. 4). The longest C–N bonds in the Cambridge Structural Database, neglecting artefacts due to disordered side chains or inaccurate structures and excluding *peri*-naphthalenes, are *ca.* 1.61 Å *e.g.* in the highly strained system **16** where the nitrogen atom is involved in the fusion of two four-membered rings and a three-membered ring.[23] Among the *peri*-naphthalenes the longest N–C bonds between *peri*-substituents are in cations **17** and **18** and zwitterion **19** and are in the range 1.66–1.68 Å.[15,17,24]

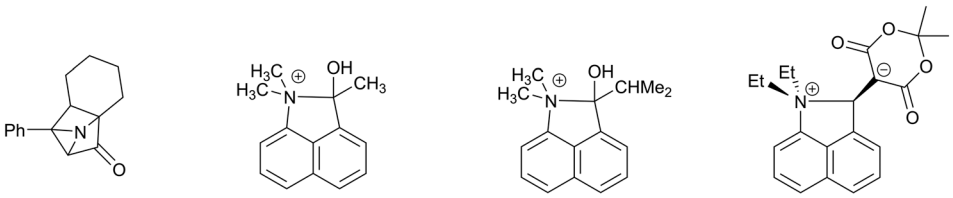

16 17 18 19

To explore this temperature dependent change of the Me_2-N···C interaction, the crystal structure of **13·Cl·0.5H$_2$O** was determined at a set of intermediate temperatures, 10 K apart, and since the most notable structural changes were found to take place between 140 and 128 K, the crystal structure was carefully measured at intervals of 2 K within this range. The crystal structure was redetermined at 132, 134, 136 and 138 K as the crystal was warmed back up to 150 K, and the results indicated that the process is reversible. The changes in the Me_2N···C separation and bond length of the C(H)═C(CN)$_2$ alkene with temperature are shown in Fig. 5 and 6. The region of fastest change with temperature is centred on *ca.* 134 K.

The overall structural change in cation **13** on cooling from 150 to 100 K is small as illustrated by the overlaid structures (Fig. 7), though significant for the two reacting groups. Two possible interpretations of the observed changes could be considered. Either there is just a steady reduction in the Me_2-N···C distance on cooling with a more rapid change in the 140 to 128 K range as the structure passes through a higher

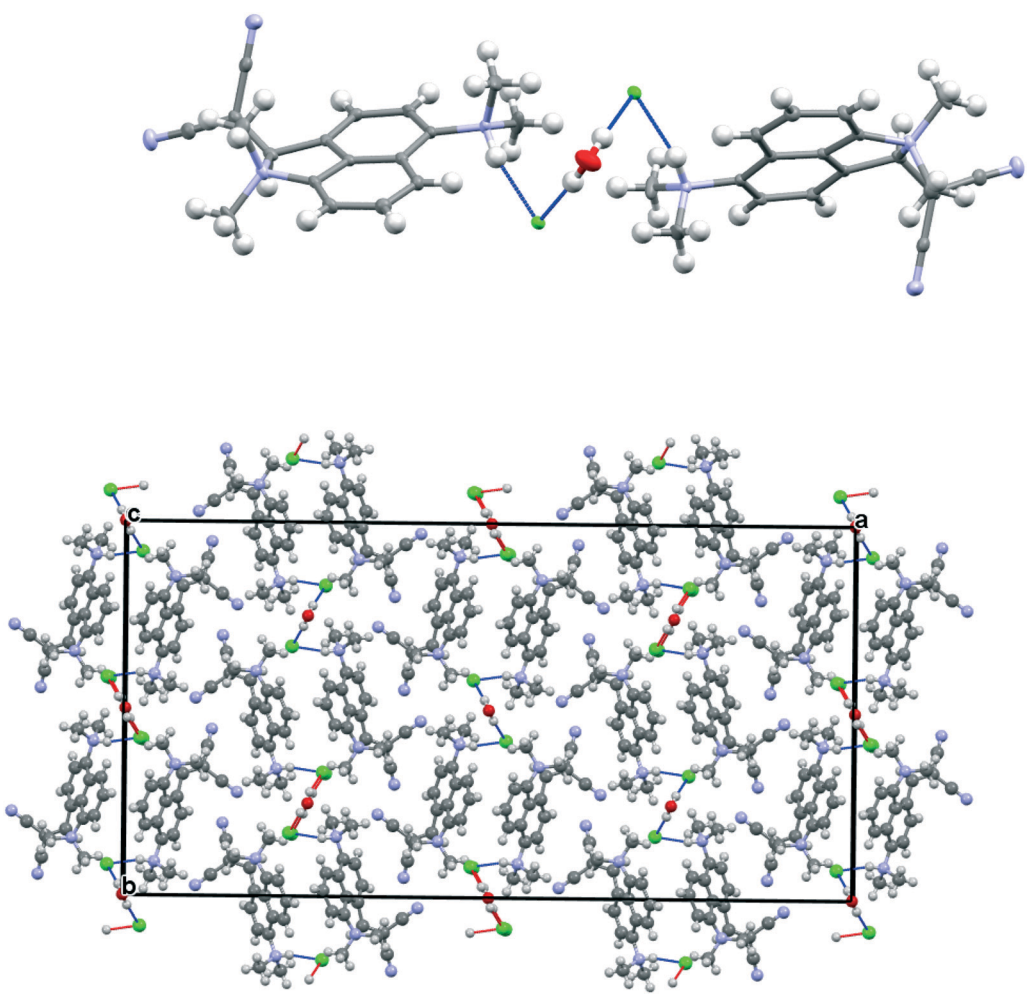

Fig. 4 Crystal packing for **13·Cl·0.5H$_2$O** at 100 K viewed down the *c* axis: a pair of chloride anions bridged by a water molecule each form a hydrogen bond to the N–H of the dimethylammmonio group of cation **13** (above) and the full crystal packing arrangement (below).

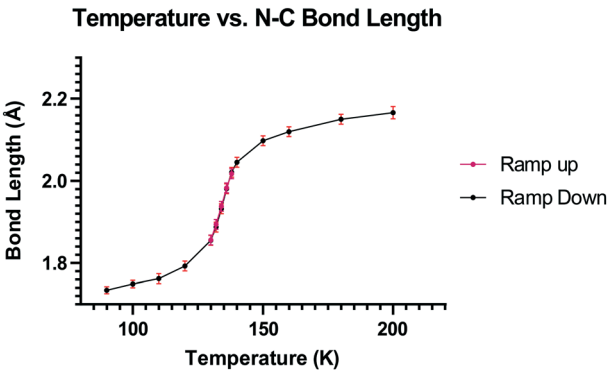

Fig. 5 Graph of the $Me_2N\cdots C$ distance (Å) *versus* temperature (K) for **13**·Cl·0.5H_2O.

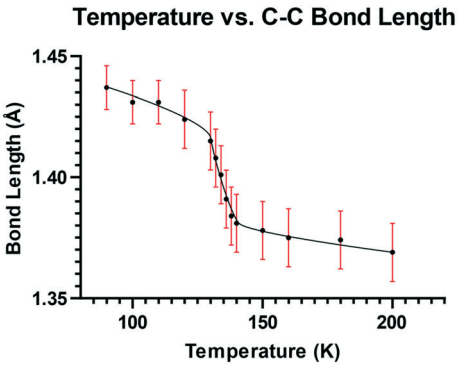

Fig. 6 Graph of the $C(H){=}C(CN)_2$ distance (Å) *versus* temperature (K) for **13**·Cl·0.5H_2O.

energy state, or there are two structures represented by those at *ca.* 140 and 128 K, and within this temperature range an increasing percentage flip over to the "128 K structure" as the temperature falls. The former interpretation would require

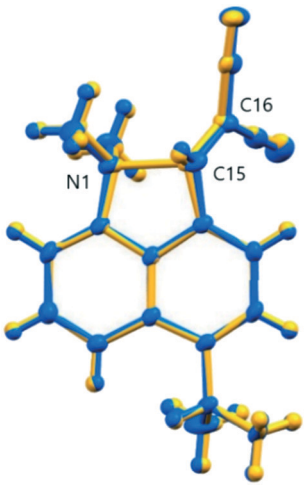

Fig. 7 An overlay of the two structures of cation **13** at 150 K (blue) and 100 K (yellow) demonstrating the changes in the overall skeleton for **13**·Cl·0.5H_2O, and selected atomic labels for those atoms most directly involved in the interaction.

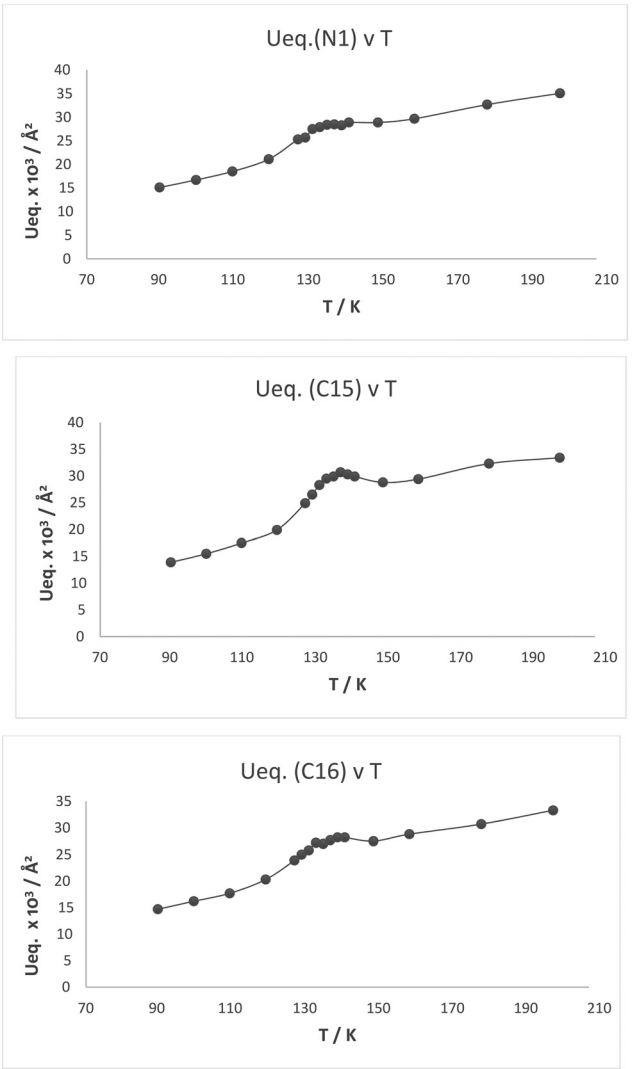

Fig. 8 Plot of $U_{eq.}$ (Å^2) against temperature (K) for the three atoms involved in the $Me_2N\cdots C(H){=}C(CN)_2$ interaction/bond formation process in cation **13**: N1, C15 and C16.

that the structure was progressing through a transition state. The latter interpretation should lead to increased atomic displacement parameters for the interacting atoms in the temperature range where a mixture of two structures was present.

Plots of the atomic $U_{eq.}$ value *versus* temperature where $U_{eq.}$ is an isotropic parameter derived from the six atomic anisotropic displacement parameters to represents the uncertainty in the atomic position due to thermal motion and/or disorder,[25] for the three atoms primarily involved in the interaction process are shown in Fig. 8. Superimposed on the expected steady decrease in the $U_{eq.}$ value with falling temperature, there is an increase which is centred at *ca.* 134 K: by *ca.* 25% for the two directly interacting atoms, the amino nitrogen N1 and the alkene carbon C15, and by *ca.* 10% for the remote alkene carbon C16 (Fig. 7). This would be consistent with the presence of two similar structural forms in this temperature range.

Structure of the cyano ester analogue, 21·Cl

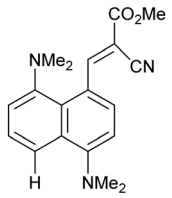

20

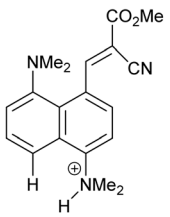

21

For comparative purposes, the corresponding methyl cyanoester **20** was prepared and converted to its chloride salt **21·Cl**. Its crystal structure was measured at 260 and 150 K. The crystal structure of this salt resembles that of the dinitrile chloride salt **13·Cl·0.5H$_2$O** in a number of respects. It includes a molecule of water per two chloride anions, and has similar cell parameters and the same space group (Fig. 9 and 10). However, the Me$_2$N···C separation in **21·Cl·0.5H$_2$O** at 260 K is 1.754(6) Å, significantly shorter than for the dinitrile salt **13·Cl·0.5H$_2$O** at 200 K (2.167(4) Å), and the partially broken alkene bond has a length of 1.442(5) *cf.* 1.369(3) Å (Table 2). Thus this structure at 260 K most closely resembles that of the dinitrile salt at 100 K. On cooling to 150 K the Me$_2$N···C separation contracts by 0.049 Å to 1.705(3) Å, and the former alkene bond extends slightly to 1.452(3) Å. So in this case, there is a substantial degree of N–C bond formation and C=C bond breaking at 260 K.

The crystal structures of the dinitrile and cyanoester salts **13·Cl·0.5H$_2$O** and **21·Cl·0.5H$_2$O** have similar orthorhombic unit cells, and the space group is *Fdd*2 in both. For the cyano ester salt, the cations are organised into columns along the *b* axis. To accommodate the ester group in place of the cyano group the *a* axis is expanded by *ca.* 9%. The *c* axis is contracted by 5%. Cations are connected in pairs by the Cl···HOH···Cl unit and are related to each other by the two fold axis through the water molecule. A second pair of cations related to the first by a 2_1 axis provides the second component of the column. However, there is a large difference in the relative orientation of the cations and the Cl···HOH···Cl unit when compared to the dinitrile salt (Fig. 10). First of all, the Cl···O···Cl angle is much wider (108.7 *cf.* 82.9°) which places the chloride ions further apart (5.310 *cf.* 4.220 Å), and the Cl···Cl vector is more closely aligned along the *b* axis lying at 9.2° *cf.* 29.2°. This pushes the two symmetry related cations further away from each other, with their protonated nitrogen atoms now 8.994 Å apart *cf.* 5.522 Å in **13·Cl·0.5H$_2$O.** This is further illustrated by the much larger Cl···O···Cl···(H)N torsion angle of 141.7 *cf.* 59.5°, though the Me$_2$N(H)···Cl···O angle remains almost constant. (91.9 *cf.* 89.1°).

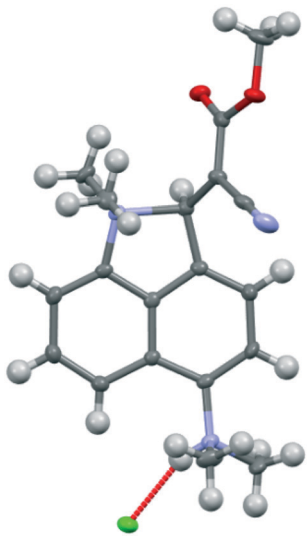

Fig. 9 Molecular structure of the cation **21** and associated chloride anion in the salt **21·Cl·0.5H$_2$O** at 150 K.

Solid state NMR studies on 13·Cl·0.5H$_2$O

To gain some further insight into the increasing progress of the reaction between the functional groups in the crystalline salt **13·Cl·0.5H$_2$O** on decreasing the temperature, the analogue which carried a ^{13}C label at the attacked alkene carbon was prepared and crystallised and then converted to a powder and studied by variable temperature solid state ^{13}C NMR. The expected unit cell dimensions were confirmed by powder X-ray diffraction The "open" analogue **3** (Me$_2$N···C: 2.413 Å) and the "closed" analogues **4** and **22–23** (Me$_2$N···C: 1.612(2)–1.651(3) Å) provide references for the chemical shift of this labelled carbon atom at its possible extreme positions: 165.6 and 88.9–99.1 ppm respectively.[16,17] In solution both the salt **13·Cl** and free base **12** show that they are in the "open" structure with the alkene carbon atoms at 163.1 and 73.4 ppm for **13·Cl** and 165.8 and 73.0 ppm for **12** in CD_2Cl_2.

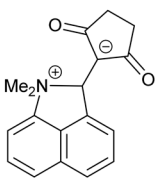

22

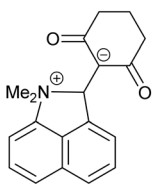

23

As pointed out above, the two possible scenarios of the structural changes on cooling should show up in the NMR spectrum in a different way. If there is just a steady reduction in the Me$_2$N···C distance on cooling, one would expect the continuous change in the chemical shift of a single line of the labelled carbon from 156 ppm to ~90 ppm. In the other scenario one would expect two lines in the spectrum corresponding to the high- and low-temperature phases, with the intensity ratio depending on the temperature. The change

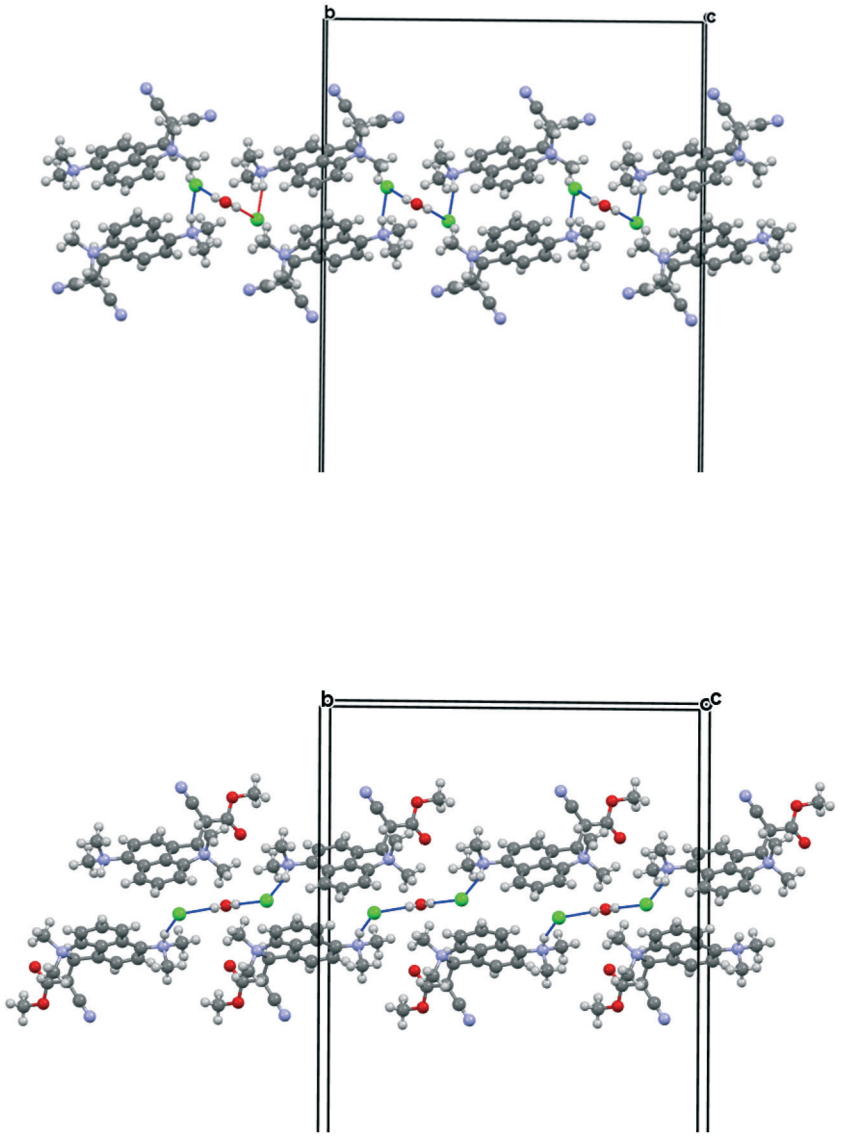

Fig. 10 Linking of pairs of cations by a Cl···HOH···Cl unit along the *b* axis for dinitrile salt **13·Cl·0.5H$_2$O** (top), and for cyanoester salt **21·Cl·0.5H$_2$O** (bottom), viewed down the *c* axis, with the *b* axis horizontal.

Table 2 Selected molecular geometry for naphthalene cation **21** in **21·Cl·0.5H$_2$O**

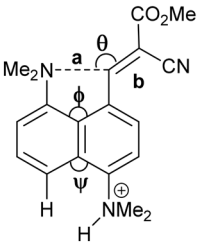

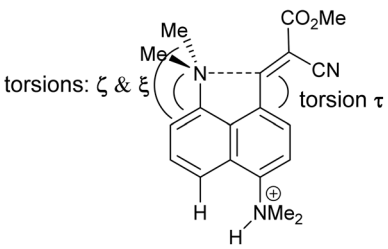

Compound	*T*/K	*a*/Å	*b*/Å	*θ*/°	Me$_2$NH···H/Å
21·Cl	260	1.754(6)	1.442(5)	115.4(3)	2.18
	150	1.705(3)	1.452(3)	115.23(18)	2.24

	T/K	*φ*/°	*ψ*/°	*τ*/°	*ζ*/°	*ξ*/°
21·Cl	260	114.2(4)	128.9(4)	46.4(6)	56.6(5)	−66.9(5)
	150	113.7(2)	129.0(2)	45.7(3)	55.7(3)	−66.7(3)

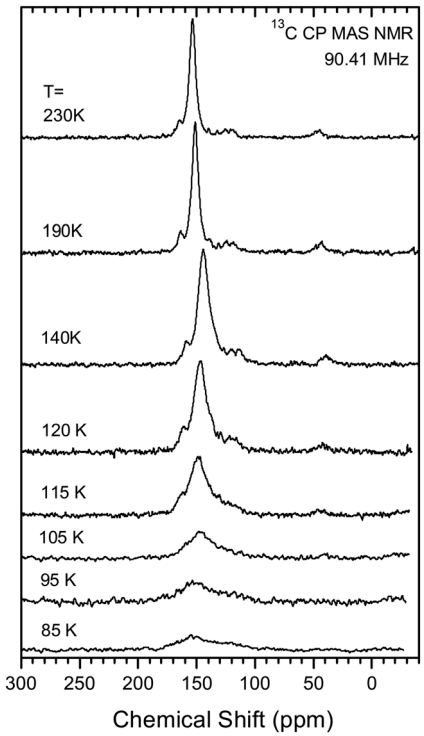

Fig. 11 Temperature dependence of ^{13}C CP MAS NMR spectrum of **13·Cl·0.5H$_2$O** sample. The details of the measurement are given in ESI.†

with temperature in the NMR spectrum of the labelled carbon is given in Fig. 11. At high temperature the spectrum shows only one signal at a chemical shift of *ca.* 153 ppm at 230 K falling to *ca.* 144 ppm at 120 K. On decreasing the temperature further, the signal amplitude decreases drastically, it becomes broader and the maximum moves back towards 150 ppm at 85 K. From this behaviour one can rule out the first scenario with a steady change in the $Me_2N\cdots C$ bond/interaction distance. Assuming coexistence of the two phases as proposed in the second scenario seems not to be fully adequate as well. The most probable explanation for such temperature dependence of the spectrum is assuming a slow exchange between the two configurations of the molecule. According to the general understanding of the NMR line shape of molecular switching between two states[26] the broadening of the line occurs when the switching rate is close to the difference of the resonances in these states. In the present case, we expect severe broadening of the line if the exchange rate between the two configurations of the molecule is of the order of few kHz.

Solution NMR studies on 13·Cl

The solution state ^{1}H and ^{13}C NMR spectra of **13·Cl** have been studied in both CD_2Cl_2 and in DMSO-d_6. In CD_2Cl_2 there appears to be a fast equilibrium between the cation **13** and the corresponding free base **12**. This leads to broadening of the ^{13}C signals *ipso*, *ortho* and *para* to the protonated NMe_2 group (Scheme 1). When not protonated electron donation into the naphthalene ring leads to upfield shifts of the *ortho* and *para* carbons and a downfield shift of the *ipso* carbon.[27] Furthermore, the two neighbouring H signals (*peri* and *ortho*) are also broadened. In DMSO-d_6 the equilibrium is more strongly towards the free base. Of further note is the upfield movement of the $-C(CN)_2$ carbon from 73.4 to 66.2 ppm on changing from CD_2Cl_2 to DMSO-d_6, consistent with an increase in electron density at this carbon. The corresponding carbanion would be expected to resonate at *ca.* 20 ppm.[28] The observed change in shift may be due to the more polar solvent stabilising a more advanced interaction between the *peri* groups. We have indeed observed a shift for the corresponding carbon at 65.5 ppm for **11** in $CDCl_3$. Interestingly the SSNMR spectrum shows this carbon at 56.5 ppm at 260 K.

Mapping of the reaction coordinate

The partial breaking of the alkene bond in cation **13**, in which it changes from a bond length of 1.369 Å at 200 K to 1.431 Å at 100 K, takes place while the $Me_2N\cdots C$ distance changes from just 2.167 Å to 1.749 Å. In the cyclised biphenyl derivative **7**, the Me_2N–C bonds are shorter (1.604(3) and 1.586(3) Å), and the "broken" alkene bonds are longer (1.487 and 1.493 Å), while in several compounds containing the $C–C^{(-)}(CN)_2$ fragment the single $C–C(CN)_2$ bond has a length in the range 1.514–1.536 Å.[29] In contrast, for the unsubstituted naphthalene **3** with a $Me_2N\cdots C$ separation of 2.413 Å, the alkene bond is 1.354 Å long. These data give insight into the bond formation and breaking in an aza-Michael reaction. For **13·Cl** at 150 K the nucleophile approaches close to the alkene ($Me_2N\cdots C$: 2.098 Å) with only a small increase of 0.024 Å in the length of double bond, but then on cooling to 100 K the alkene bond is partially broken while the $Me_2N\cdots C$ distance contracts by just 0.349 Å. To get a fuller picture of this correlation the corresponding distances from a

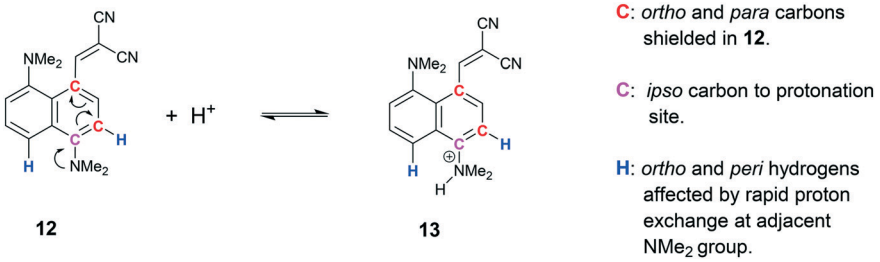

Scheme 1 Equilibrium of cation **13** with free base **12** observed in solution by NMR.

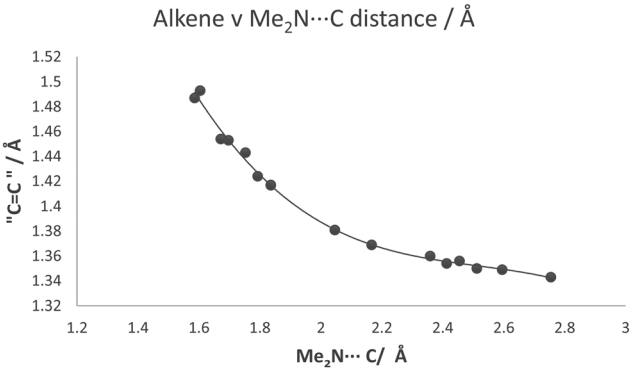

Fig. 12 For a series of compounds containing the $Me_2N\cdots C(H)=C(CN)_2$ grouping, a plot of the length of approached alkene bond against $Me_2N\cdots C$ separation.

range of structures containing an interaction or bond between a dimethylamino group and an ethene-2,2-dinitrile (**3**, **7**, **8**, **11**, **12**, **13**@200 K, **13**@150 K, **13**@140 K, **13**@128 K, **13**@120 K, **13**@100 K) are plotted in Fig. 12, from a $Me_2N\cdots C$ separation of *ca.* 2.8 Å in acenaphthene **8** to *ca.* 1.6 Å in the biphenyl **7**. We also included three data points where one of the nitriles is replaced by a methyl ester, two from **18·Cl** (@260 K and 150 K) and also the corresponding *peri*-naphthalene with no extra *peri* substituents **24** (ESI†). The graph shows a curved correlation, though of course it is short of data in the range 1.75–2.01 Å.

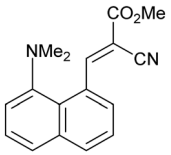

24

Goodman's calculations on the transition state for attack by methylamine on acrolein and acrylamide where the double bond is activated by an aldehyde or a primary amide group show $MeN(H_2)\cdots C$ contacts of 2.04 and 1.84 Å, and alkene bond lengths of 1.393 and 1.412 Å respectively.[5] From our crystallographic data, where the reaction is intramolecular and thus the product has the additional consideration of strain energy due to formation of a fused ring, a very approximate estimate for the position of the transition state from the crystallographic data could be the mid-point of the zone in which the $Me_2N\cdots C$ distance changes quickly, *i.e.* with a $Me_2N\cdots C$ separation of *ca.* 1.94 Å and the former C=C bond at *ca.* 1.40 Å.

Conclusion

This study provided insight into the correlation between the bond breaking and bond formation processes in an aza-Michael reaction using groups positioned at the *peri*-positions of a naphthalene ring, with their separation modified by steric interactions at the opposite *peri*-positions. An ethylene bridge leads to increased separation while repulsion between two phenyl groups leads to decreased separation. Having established the principle, then further compression between the reactive groups can be attempted using larger substituents. Of particular interest is the reversible behaviour with temperature of the naphthalene based salt **13·Cl·0.5H$_2$O** in which the $Me_2N\cdots C$ separation closes from 2.167 to 1.749 Å on cooling from 200 to 100 K. The balance of evidence currently suggests that there is a dynamic equilibrium between two close structural forms in the range 140–128 K. Using the Pauling expression for bond order, at 200 K the *peri* N···C interaction corresponds to a bond order of *ca.* 0.15, while at 100 K the bond order is *ca.* 0.47,[30] though these may be underestimates since the formula applies to bond between neutral atoms. Further investigations are warranted, including charge density measurements by accurate X-ray diffraction at different temperatures on this material and closely related salts, a structural study of the effect of externally applied pressure on the separation between the reactive groups as well as appropriate calculations and spectroscopic investigations. Single crystal to single crystal phase transitions are well known in molecular materials, though usually involve the reorientation of the molecules relative to each other and reorganisation of the attractive interactions between them.[31] In contrast, the case discussed here involves just a step change in the close *intramolecular* interaction/partial bond formation between two groups, and is very rare. Crystallographic studies suggest that at the lower limit (1.75 Å) there is some form of bond between the reactive groups, given the strong induction of pyramidality at the carbon atom and extension of the alkene bond, though it may be more appropriate to consider this a partially formed bond. Charge density studies may provide further insight into this. Only a few N···C separations in this range are known, in particular in systems with a transannular N···C=O interaction: clivorine **5** with a N···C separation of 1.993(3) Å and a somewhat lengthened C=O bond (1.258(3) Å), and senkirkine **6** where the N···C separation is longer (2.293 Å) but the carbonyl bond in the usual range (1.213 Å).[18] Just why the cation **13** can tolerate the higher energy interactions between functional groups in the 2.2–1.7 Å region may be due to the role of strong hydrogen bonding stabilising this particular type of crystal structure.

Experimental

Full details of the synthesis and characterisation of new substances, the determination of crystal structures by X-ray diffraction, solid-state NMR studies and calculations are provided in the ESI.† Crystal structures have been deposited at the Cambridge Structural Database with numbers: CCDC 2016747–2016754 and 2019629.

Conflicts of interest

There are no conflicts of interest to report.

Acknowledgements

We thank Nottingham Trent University for a studentship (JCB) and for financial support for materials. We wish to thank Dr Tõnis Pehk for additional assignment of the solution NMR resonances. I. H. and R. S. were supported by the European Regional Development Fund (Grant No. TK134), and by the Estonian Research Council (PRG4, IUT23-7).

References

1 J. C. Polanyi and A. H. Zewail, *Acc. Chem. Res.*, 1995, **28**, 119–122; D. Zhong and A. R. Zewail, *J. Phys. Chem. A*, 1998, **102**, 4031–4058; A. R. Attar, A. Bhattacherjee and S. R. Leone, *J. Phys. Chem. Lett.*, 2015, **8**, 5072–5077; A. A. Ischenko, P. M. Weber and R. J. D. Miller, *Russ. Chem. Rev.*, 2017, **86**, 1173–1253.

2 L. D. Jacobson, A. D. Bochevarov, M. A. Watson, T. F. Hughes, D. Rinaldo, S. Ehrlich, T. B. Steinbrecher, S. Vaitheeswaran, D. M. Philipp, M. D. Halls and R. A. Friesner, *J. Chem. Theory Comput.*, 2017, **13**, 5780–5797; A. B. Birkholz and H. B. Schlegel, *J. Comput. Chem.*, 2015, **36**, 1157–1166; L. K. Beland, P. Brommer, F. El-Mellouhi, J.-F. Joly and N. Mousseau, *Phys. Rev. E*, 2011, **84**, 046704.

3 M. B. Smith, *March's Advanced Organic Chemistry*, John Wiley and Sons Inc., New Jersey, 8th edn, 2020; P. Wadhu, A. Kharbanda and A. Sharma, *Asian J. Org. Chem.*, 2018, **7**, 634–661; C. F. Nising and S. Bräse, *Chem. Soc. Rev.*, 2012, **41**, 988–999; C. F. Nising and S. Bräse, *Chem. Soc. Rev.*, 2008, **37**, 1218–1228; R. D. Little, M. R. Masjedizadeh, O. Wallquist and J. I. McLoughlin, *Org. React.*, 1995, **47**, 315–552.

4 R. W. Bates, W. Ko and V. Barát, *Org. Biomol. Chem.*, 2020, **18**, 810–829; M. G. Vinogradov, O. V. Turova and S. G. Zlotin, *Org. Biomol. Chem.*, 2019, **17**, 3670–3708; M. Sánchez-Roselló, J. L. Aceña, A. Simón-Fuentes and C. Del Pozo, *Chem. Soc. Rev.*, 2014, **43**, 7430–7453; Z. Amara, J. Caron and D. Joseph, *Nat. Prod. Rep.*, 2013, **30**, 1211–1225; A. Y. Rulev, *Russ. Chem. Rev.*, 2011, **8**, 197–218.

5 T. E. H. Allen, M. N. Grayson, J. M. Goodman, S. Gutsell and P. J. Russell, *J. Chem. Inf. Model.*, 2018, **58**, 1266–1271.

6 J. A. Izzo, Y. Myshchuk, J. S. Hirschi and M. J. Vetticatt, *Org. Biomol. Chem.*, 2019, **17**, 3934–3939; S. Romanini, E. Galletti, L. Caruana, A. Mazzanti, F. Himo, S. Santoro, M. Fochi and L. Bernardi, *Chem. – Eur. J.*, 2015, **21**, 17578–17582; E. H. Krenske, R. C. Petter, Z. Zhu and K. N. Houk, *J. Org. Chem.*, 2011, **76**, 5074–5081; D. Mulliner, D. Woudrousch and G. Schüürmann, *Org. Biomol. Chem.*, 2011, **9**, 8400–8412; J. A. H. Schwöbel, J. C. Madden and M. T. D. Cronin, *SAR QSAR Environ. Res.*, 2010, **21**, 693–710; E. E. Kwan and D. A. Evans, *Org. Lett.*, 2010, **12**, 5124–5127.

7 *Structure Correlation*, ed. H.-B. Bürgi and J. D. Dunitz, VCH, Weinheim, 1994, vol. 1; E. Hupf, M. Olaru, C. I. Rat, M. Fugel, C. B. Hübschle, E. Lork, S. Grabowsky, S. Mebs and J. Beckmann, *Chem. – Eur. J.*, 2017, **23**, 10568–10579.

8 J. C. Bristow, M. A. Addicoat and J. D. Wallis, *CrystEngComm*, 2019, **21**, 1009–1018; F. R. Knight, R. A. M. Randall, K. S. Athukorala Arachchige, L. Wakefield, J. M. Griffin, S. E. Ashbrook, M. Bühl, A. M. Z. Slavin and J. D. Woolins, *Inorg. Chem.*, 2012, **51**, 11087–11097; K. S. M. Mickoleit, R. Kempe and H. Oehme, *Angew. Chem., Int. Ed.*, 2000, **39**, 1610–1612; G. P. Schiemenz, *Z. Naturforsch., B: J. Chem. Sci.*, 2006, **61**, 535–554.

9 K. Yamamoto, N. Oyamada, S. Xia, Y. Kobayashi, M. Yamaguchi, H. Maeda, H. Nishihara, T. Uchimaru and E. Kwon, *J. Am. Chem. Soc.*, 2013, **135**, 16526–16532.

10 D. Pla, O. Sadek, S. Cadet, B. Mestre-Voegtlé and E. Gras, *Dalton Trans.*, 2015, **44**, 18340–18346.

11 H. A. Staab and T. Saupe, *Angew. Chem., Int. Ed. Engl.*, 1988, **27**, 865–879.

12 S. Sarkar and T. N. Guru Row, *IUCrJ*, 2017, **4**, 37–49; P. R. Mallinson, G. T. Smith, C. C. Wilson, E. Grech and K. Wozniak, *J. Am. Chem. Soc.*, 2003, **125**, 4259–4270.

13 W. B. Schweizer, G. Procter, M. Kaftory and J. D. Dunitz, *Helv. Chim. Acta*, 1978, **61**, 2783–2808.

14 A. Wannebroucq, A. P. Jarmyn, M. B. Pitak, S. J. Coles and J. D. Wallis, *Pure Appl. Chem.*, 2016, **88**, 317–331.

15 N. Mercadal, S. P. Day, A. Jarmyn, M. B. Pitak, S. J. Coles, C. Wilson, G. J. Rees, J. V. Hanna and J. D. Wallis, *CrystEngComm*, 2014, **16**, 8363–8374.

16 P. C. Bell and J. D. Wallis, *Chem. Commun.*, 1999, 257–258.

17 A. Lari, M. B. Pitak, S. J. Coles, G. J. Rees, S. P. Day, M. E. Smith, J. V. Hanna and J. D. Wallis, *Org. Biomol. Chem.*, 2012, **10**, 7763–7779; J. O'Leary, W. Skranc, X. Formosa and J. D. Wallis, *Org. Biomol. Chem.*, 2005, **3**, 3273–3283.

18 K. B. Birnbaum, *Acta Crystallogr., Sect. B: Struct. Crystallogr. Cryst. Chem.*, 1972, **28**, 2825–2833; G. I. Birnbaum, *J. Am. Chem. Soc.*, 1974, **96**, 6165–6168.

19 H.-B. Bürgi, J. D. Dunitz and E. Schefter, *J. Am. Chem. Soc.*, 1973, **95**, 5065–5067.

20 R. W. Newberry and R. T. Raines, *Acc. Chem. Res.*, 2017, **50**, 1838–1846; R. W. Newberry, G. J. Bartlett, B. VanVeller, D. N. Woolfson and R. T. Raines, *Protein Sci.*, 2014, **23**, 284–288.

21 J. O'Leary and J. D. Wallis, *Org. Biomol. Chem.*, 2009, **7**, 225–228.

22 Y. Ishigaki, T. Shimajiri, T. Takeda, R. Takoono and T. Suzuki, *Chem*, 2018, **4**, 795–806.

23 S. Pusch, D. Schollmeyer and T. Opatz, *Exp. Cryst. Struct. Determ.*, 2016, REFCODE: UTOBUC.

24 I. I. Schuster, A. J. Freyer and A. L. Rheingold, *J. Org. Chem.*, 2000, **65**, 5752–5759.

25 R. X. Fischer and E. Tillmans, *Acta Crystallogr., Sect. C: Cryst. Struct. Commun.*, 1988, **44**, 775–776.

26 C. P. Slichter, *Principles of Magnetic Resonance*, Springer-Verlag, 3rd edn, 1992, p. 596.

27 D. Škalamera, L. Cao, L. Isaacs, R. Glaser and K. Mlinarić-Majerski, *Tetrahedron*, 2016, **72**, 1541–1546.

28 W. F. Richter, K. Hartke, W. Massa and G. Münninghof, *Chem. Ber.*, 1989, **122**, 1133–1137.

29 H. Song, Y. Kim, J. Park, Y. H. Ko and E. Lee, *Eur. J. Org. Chem.*, 2017, 1231–1235; L. Carlucci, G. Ciani, D. M. Proserpio and A. Sironi, *Angew. Chem., Int. Ed. Engl.*, 1996, **35**, 1088–1090; REFCODES: KANZUX, NACVOC, NACVUI, ULAVAG; M. Y. Belikov, M. Y. Ievlev, I. V. Belikova, O. V. Ershov, V. A. Tafeenko and M. D. Surazhskaya, *Chem. Heterocycl. Compd.*, 2015, **51**, 518–525.

30 N. E. Brese and M. O'Keefe, *Acta Crystallogr., Sect. B: Struct. Sci.*, 1991, **47**, 192–197; I. D. Brown, 2016, https://www.iucr.org/resources/data/datasets/bond-valence-parameters, (accessed July 2020); L. Pauling, *The Nature of the Chemical Bond and the Structure of Molecules and Crystals: An Introduction to Modern Structural Chemistry*, Cornell University Press, New York, USA, 1960.

31 V. K. Srirambhatla, R. Guo, D. M. Dawson, S. L. Price and A. Florence, *Cryst. Growth Des.*, 2020, **20**, 1800–1810; M. M. H. Smets, E. Kalkman, A. Krieger, P. Tinnemans, H. Meeks, E. Vlieg and H. M. Cuppen, *IUCrJ*, 2020, **7**, 331–341; C. Ge, J. Liu, X. Ye, Q. Han, L Zhang, S. Cui, Q. Guo, G. Liu, Y. Liu and X. Tao, *J. Phys. Chem. C*, 2018, **122**, 15744–15752; R. Enjalbert and J. Galy, *Acta Crystallogr., Sect. B: Struct. Sci.*, 2002, **58**, 1005–1010.